

## Liquid Membrane Electrochemical Etching: Twin Nano-Tips Fabrication for Micromachining

Yufeng Wang<sup>1</sup>, Yongbin Zeng<sup>1,2,\*</sup>, Xiaofeng Wang<sup>1</sup>, Ningsong Qu<sup>1,2</sup>, Di Zhu<sup>1,2</sup>

<sup>1</sup> College of Mechanical and Electrical Engineering, Nanjing University of Aeronautics and Astronautics, Nanjing, China, 210016

<sup>2</sup> Jiangsu Key Laboratory of Precision and Micro-Manufacturing Technology, Nanjing, China, 210016

\*E-mail: [binyz@nuaa.edu.cn](mailto:binyz@nuaa.edu.cn)

Received: 24 December 2015 / Accepted: 21 February 2016 / Published: 1 April 2016

---

Nano-electrodes are essential components in electrochemical micromachining, allowing high machining accuracy and minimum machining size. Liquid membrane electrochemical etching processes twin nano-electrodes with parabolic upper and conical lower nano-electrodes simultaneously. After the lower tip drops off, blunting due to residual current increases the diameter of the upper tip. This blunting can be decreased by cutting off the residual current in 5 ms with a newly developed control strategy. Experimental results indicate that the diameters of both nano-electrodes decrease with the use of lower voltage and electrolyte concentration and shorter lower-end length. To avoid low etching efficiency or a boiling effect, appropriate parameters should be selected. Blunting can also be reduced by using lower voltage and electrolyte concentration. Twin nano-electrodes with upper- and lower-tip diameters of 110 and 80 nm, respectively, have been fabricated and used to make micro-holes of 2  $\mu\text{m}$  diameter by electrochemical micro-drilling.

---

**Keywords:** Electrochemical etching; Liquid membrane; Nanoelectrode; Blunting; Cut off

### 1. INTRODUCTION

With the trend toward miniaturization in various fields, there is an increasing demand for micro- and nano-scale components or complete devices [1]. Micro electro mechanical systems (MEMS), for instance, have been introduced into automobiles, smart devices, aircrafts, unmanned aerial vehicles, etc. Therefore, processes for micro- and nanofabrication are required. Various methods have been studied for micro- and nano-scale manufacturing, including micromechanical machining, energy-beam machining, lithography, and electro-physical and electrochemical processes [2-4].

Electrochemical machining has been applied as a micromachining process because of its mechanism of removing material by anodic dissolution. It is a process that does not introduce thermal or mechanical stress [5]. Schuster et al. [6] studied electrochemical micromachining with ultrashort voltage pulses and showed that the machining precision could be improved to a sub-micrometer scale. Trimmer et al. [7] processed complex nanostructures by electrochemical micromachining with shaped tungsten tools. Kock et al. [8] etched 1  $\mu\text{m}$  deep micro-trenches with a spatial resolution less than 100 nm using a tool electrode with a radius of about 45 nm. Ahn et al. [9] fabricated micro-holes 8  $\mu\text{m}$  in diameter by electrochemical micro drilling using a 6  $\mu\text{m}$  diameter micro-tool electrode. Ghoshal and Bhattacharyya [10] processed micro-profiles and micro-channels using straight, conical, and reversed-taper micro-tools. The results of these studies indicate that the tool electrode plays a crucial role in electrochemical micromachining. Both the scale and accuracy of tool electrodes are closely related to the machining precision and the achievable minimum sizes. Bhattacharyya et al. [11] showed that suitable preparation of micro-tools is necessary for successful machining.

Micro- and nano-electrodes have been widely prepared by electrochemical etching without drawbacks such as surface cracks, residual stress, and deformations [12]. Ibe et al. [13] reported a direct-current drop-off electrochemical etching procedure to prepare sharpen tips with radius of curvature varied from 20 to greater than 300 nm. Khan et al. [14] and Ge et al. [15] produced tungsten tips with a radius of curvature less than 10 nm by dynamic electrochemical etching. Mihim and Mrad [16] proposed an electrochemical etching technique that combined static and dynamic etching processes to fabricate well-defined conical tips of length 2 mm and radius 20 nm. Chen et al. [17] presented an efficient electrochemical etching technique with constant-current mode to fabricate Ni tips. Lim and Kim [18] fabricated a thin cylindrical micro-pin with a diameter of 50  $\mu\text{m}$  and a length of 4 mm by adjusting the current and voltage during electrochemical etching. Liquid membrane electrochemical etching has also been used to fabricate nano-electrodes. Zeng et al. [19] and Wu et al. [20] used liquid membrane electrochemical etching to prepare nano-electrodes with diameters of about 85 nm. Wang et al. [21] applied a straight reciprocating motion to the anodic rod during liquid membrane electrochemical etching to produce high-aspect-ratio nano-electrodes. However, with liquid membrane electrochemical etching, only one nano-electrode of conical or cylindrical shape is obtained, because the end of the upper tip is blunted after the anode breaks off. In addition, to date, there have not been any studies of control programs for the process.

In this paper, liquid membrane electrochemical etching is used to prepare twin nano-electrodes with a parabolic upper tip and conical lower tip. The current during etching is monitored to allow control of the process. A sudden drop in current occurs when the anodic rod breaks and the lower tip drops off. The current should then be cut off as quickly as possible to prevent blunting of the upper tip and thus obtain two nano-electrodes simultaneously. Experimental results indicate that the diameter of the upper tip increases rapidly with the time delay between the lower tip breaking away and the current being cut off. Using the control strategy developed here, the effects of different parameters such as applied voltage, electrolyte concentration, lower-end length, and cut-off time on the diameter of the twin nano-electrodes are investigated. The results reveal that small values of these parameters are preferred for fabricating twin nano-electrodes of smaller sizes and for decreasing the blunting effect.

## 2. EXPERIMENTAL

### 2.1 Setup and principles of liquid membrane electrochemical etching

As shown in figure 1, a tungsten rod (0.3 mm diameter, Goodfellow) passes through a cathode ring (8 mm diameter) holding a liquid membrane of thickness 4 mm formed from potassium hydroxide (KOH) solution. The tungsten rod is fixed in a spindle (NR2551, NSK) mounted on the X-Y-Z motion platform (M511.DG, PI), and the cathode ring is fixed in perpendicular to the Z-axis. The tungsten rod and the ring are connected to the positive and negative polarities, respectively, of a voltage source (IT6421, ITECH). When the voltage is turned on, material is selectively removed from the tungsten rod within the liquid membrane through the following electrochemical reactions:

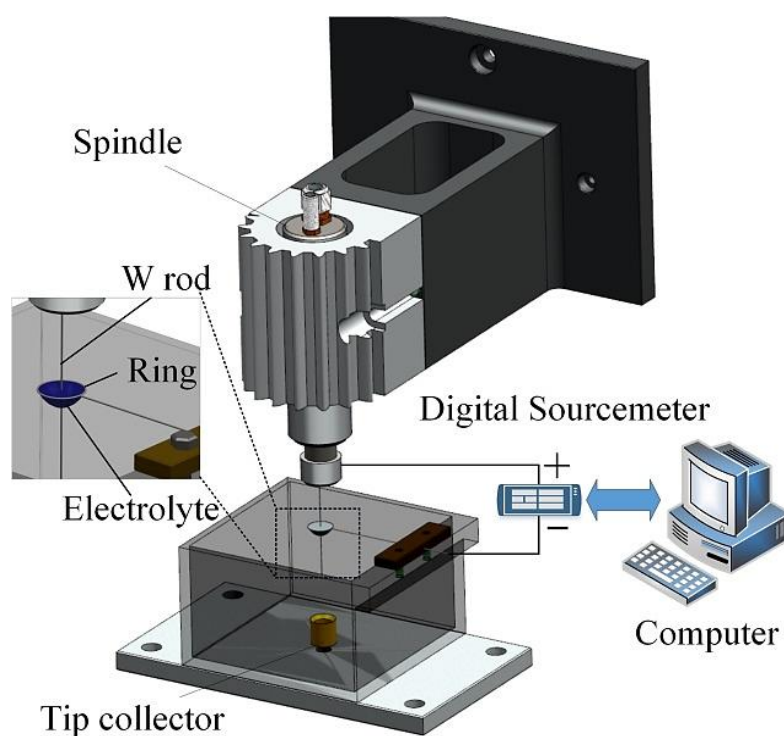
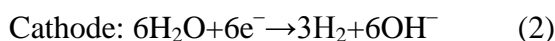


**Figure 1.** Apparatus for liquid membrane electrochemical etching of twin nano-electrodes.

The diameter of the tungsten rod within the liquid membrane decreases with etching time, as shown in figure 2(a). The diameter is smallest at the interface between air and electrolyte, where the current density is greatest. The upper tip is parabolic owing to the shape of the meniscus, whereas the lower tip takes on a sharp conical shape owing to the formation of a diffusion layer around the rod. Thus, a necking is formed on the rod. Finally, the rod breaks owing to the tensile failure caused by the force of gravity on its lower end, while the diameter of the necking decreases to a very small value. As a result, twin nano-electrodes are prepared simultaneously.

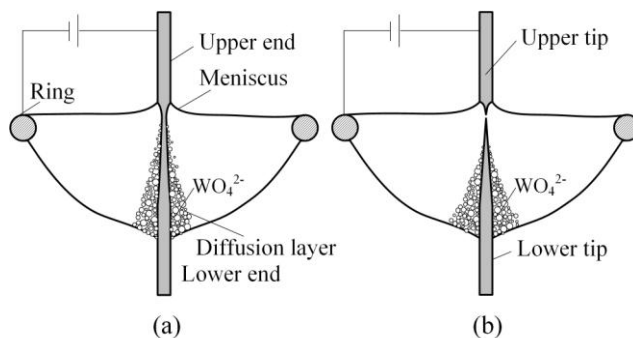


**Figure 2.** Etching of the tungsten rod: (a) decrease in anodic rod diameter; (b) the rod breaks and its lower tip drops off under the force of gravity.

2.2 Process monitoring with etching current

Figure 3 shows evolution of the etching current during liquid membrane electrochemical etching. The current was measured by the voltage source and was transmitted to a computer for post-processing. The steep increase in current during the initial stage indicates the beginning of the etching process. The current then decreases steadily with time before the tungsten rod breaks. This decrease is due to consumption of electrolyte ions and the decrease in diameter of the rod. In the final stage of the process, there are two sudden drops in the etching current. The first of these indicates the breakage of the tungsten rod, and the second occurs when the current is cut off. Thus, the current does not disappear immediately after the tungsten rod breaks; that is, a residual current continues to exist before the current is switched off. Figure 4 shows photographs of the breakage of the tungsten rod obtained by a CCD camera (GRAS-S50S5C, Point Grey Research). It reveals that the upper tip is still immersed in the electrolyte after the lower tip drops off, which is the cause of the residual current. It is this electrolytic action of this residual current that is responsible for the blunting of the upper tip.

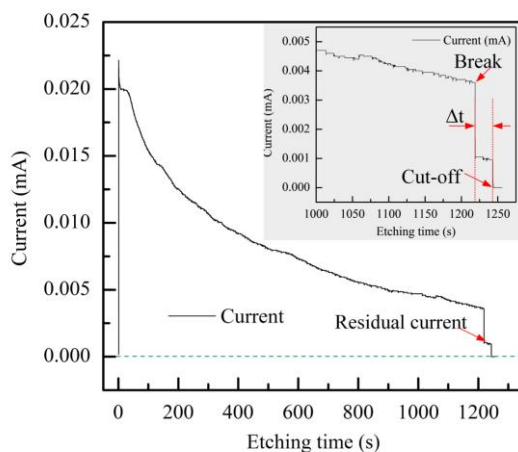


**Figure 3.** Evolution of the etching current during liquid membrane electrochemical etching. The first sudden drop indicates the breakage of the tungsten rod, and the second indicates the cut-off of the current.  $\Delta t$  denotes the time delay between the rod breaking and the current being switched off.

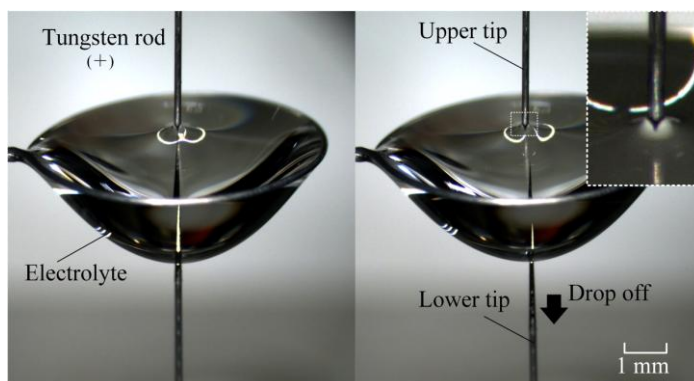


**Figure 4.** Photographs of the breakage of the tungsten rod. It can be seen that the upper tip is still immersed in electrolyte after the lower tip drops off.

In principle, the upper and lower tips should be identical in diameter. However, the upper tip is blunted by continuing electrolytic dissolution after the lower tip drops off, whereas the etching of the lower tip stops instantly after the rod breaks. Thus, the diameter of the upper tip is always greater than that of the lower tip. In order to prepare twin nano-electrodes, the time delay before the current is switched off,  $\Delta t$ , should be as small as possible to reduce the blunting of the upper tip.

### 2.3 Process control program

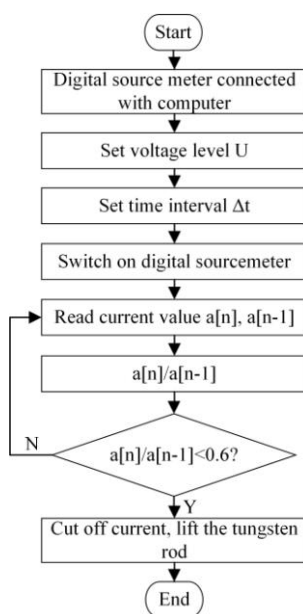


**Figure 5.** Control flow for liquid membrane electrochemical etching of twin nano-electrodes.

During the etching process, the current value is acquired by a digital source meter (IT6121, ITECH) that is connected to a computer via a universal serial bus. A Labview program has been developed for acquiring and analyzing the current value  $a[n]$ . The variation ratio  $a[n]/a[n-1]$  is utilized

to indicate the state of the liquid membrane electrochemical etching process. Breakage of the tungsten rod is detected if  $a[n]/a[n-1] < \alpha$  ( $\alpha = 0.6$ ). Figure 5 shows the control program for detecting the breakage of the tungsten rod and switching off the current. When the rod breaks, the current is shut off immediately and the upper tip is lifted from the electrolyte. With this control procedure, the time for cutting off the residual current is about 5 ms. This reduces the blunting of the upper tip. After etching, both the upper and lower tips are measured by SEM (S3400, Hitachi).

### 3. RESULTS AND DISCUSSION

#### 3.1 Cut-off time and blunting effect

The feasibility of the proposed method is investigated for both of the nano-electrodes with cut-off times of 5, 15, 30, and 60 s compared with the time of 5 ms in the proposed procedure. An applied voltage of 4 V, an electrolyte concentration of 2 mol/L, and a lower-end length of 15 mm were used during liquid membrane electrochemical etching of the twin nano-electrodes. Figure 6 shows the evolution of the etching current and the variation ratio  $a[n]/a[n-1]$  while the developed control program was applied. It proves that this program could detect the breakage of the tungsten rod and immediately cut off the residual current.

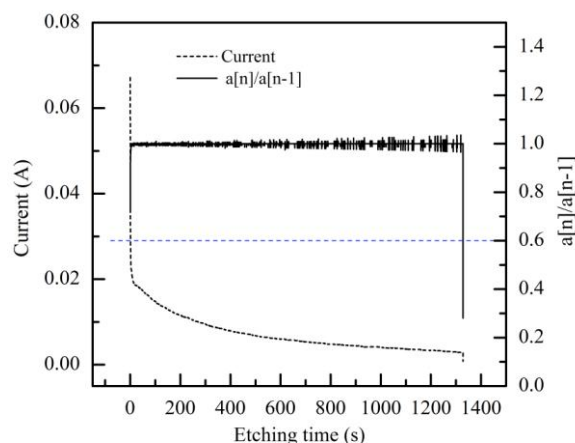


**Figure 6.** Evolution of the etching current and the variation ratio  $a[n]/a[n-1]$ . A value of  $a[n]/a[n-1] < 0.6$  indicates breakage of the tungsten rod.

As can be seen in figure 7, the diameters of the processed lower tips were about 90 nm. However, the upper tip is rapidly blunted with increasing delay in cutting off the current. Figure 8 shows that the diameter of the upper tip was 170 nm with a cut-off time of 5 ms, and increased to 320 nm as the cut-off was delayed by 5 s. Ibe et al. also demonstrated that a minimum cut-off time is required for producing nano tips with smaller radius of curvature [13].

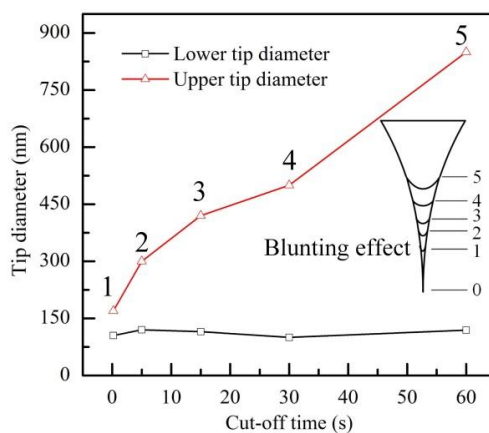


**Figure 7.** Influence of cut-off time on the tip diameters of the upper and lower nano-electrodes.

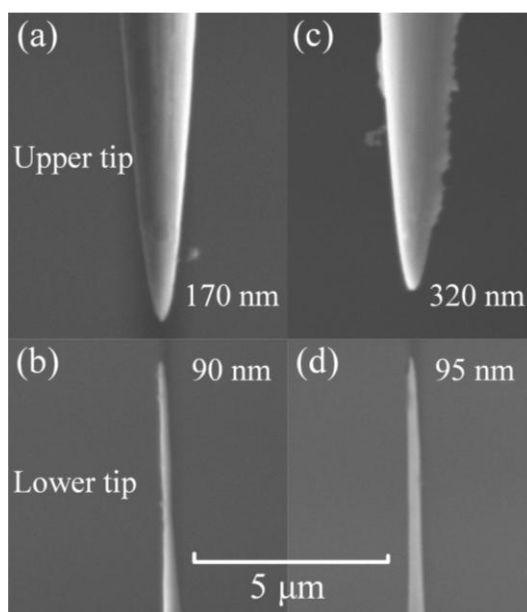


**Figure 8.** Upper and lower nano-electrodes processed by liquid membrane electrochemical etching with cut-off times of (a), (b) 5 ms, and (c), (d) 5 s.

### 3.2 Voltage and twin nano-electrodes

Using the proposed method with a fast cut-off of the residual current, the effects of various applied voltages ranging from 3 to 10 V on the processing of both of the nano-electrodes were studied. An electrolyte concentration of 2 mol/L, tungsten rod diameter of 0.3 mm, and lower-end length of 15 mm were adopted. As shown in figure 9, both the upper and lower tips increased in diameter with increasing applied voltage. Under a larger applied voltage, the increased material removal rate (volume removed per unit time) causes over-etching of the tip radius when the tungsten rod breaks. Moreover, the difference between upper- and lower-tip diameters increased with voltage, owing to the growth of

residual current. With the increasing residual current, the blunting of the upper tip is enhanced, causing the increased upper-tip diameter. Therefore, with a lower applied voltage, smaller upper and lower nano-electrodes could be fabricated by liquid membrane electrochemical etching. Wu et al. also reported that the diameter of the lower tip decreases with decreasing applied voltage [20], but the upper tips were not studied in their research.

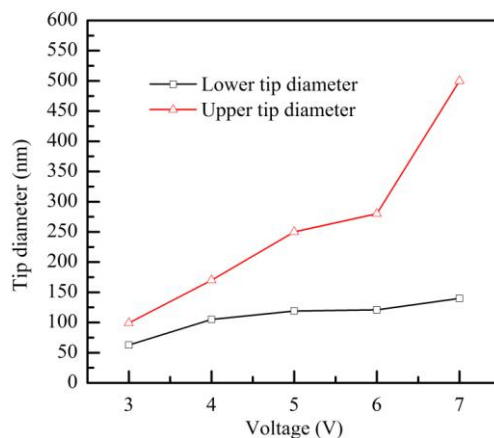


**Figure 9.** Influence of applied voltage on processed upper and lower nano-electrodes.

It was also found that applied voltages between 3 and 7 V should be used under the given conditions. With smaller voltages, the processing efficiency is very low: the required etching time with a voltage of 2 V was more than 2 hours. However, when the voltage is greater than 7 V, a “boiling” effect occurs in the electrolyte, similar to the boiling of a liquid. The significant increase in etching rate at higher voltages leads to the generation of a large amount of hydrogen gas at the cathode, and this disrupts the liquid membrane, causing the current to increase in an unstable manner, as shown in figure 10. The liquid membrane is destroyed and falls from the cathode ring, and so the etching can no longer continue.

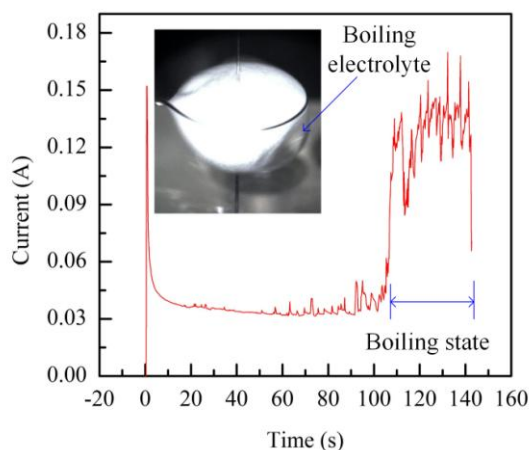


**Figure 10.** Etching current at an applied voltage greater than 7 V, and the inserted picture shows the boiling electrolyte on the boiling state.



### 3.3 Electrolyte concentration and twin nano-electrodes

Figure 11 shows the effect of electrolyte concentration on both tips at an applied voltage of 4 V, with a lower-end length of 15 mm. The experimental results revealed that an electrolyte concentration of 1.5 to 3 mol/L is preferred for the fabrication of nano-electrodes. Low etching efficiency and a boiling effect were also observed at low and high electrolyte concentrations, respectively. Both the upper- and lower-tip diameters grew as the etching rate increased with increasing electrolyte concentration. Moreover, the blunting of the upper tip was enhanced by the increased residual current. The results showed residual currents of 15, 25, 50, and 80 mA at electrolyte concentrations of 1.5, 2, 2.5, and 3 mol/L, respectively.

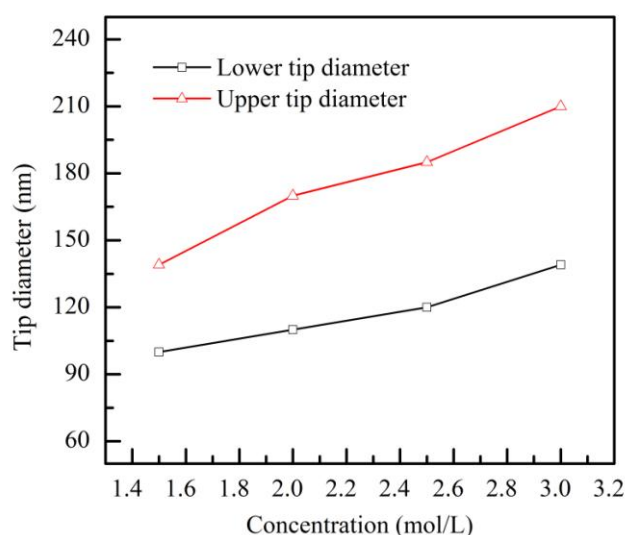


**Figure 11.** Influence of electrolyte concentration on prepared upper and lower nano-electrodes.

### 3.4 Lower-end length and twin nano-electrodes

The lower-end length (the length of tungsten rod below the cathode ring) determines the weight of the lower end at a given rod diameter. Obviously, the weight of the lower end increases with increasing length, causing the rod to break at a large diameter. Thus, both the upper- and lower-tip diameters increase with increasing lower-end length, which is in accordance with the experimental results shown in figure 12, which also indicates that the difference between upper- and lower-tip diameters remains almost constant. This is because the blunting effect is the same under the same residual current, at identical applied voltage and electrolyte concentration. Zeng et al. has also studied the effects of acting force on the lower end of the tungsten rod, and indicated that a smaller force on the lower end is helpful to fabricate nano tips with smaller tip radius [22].

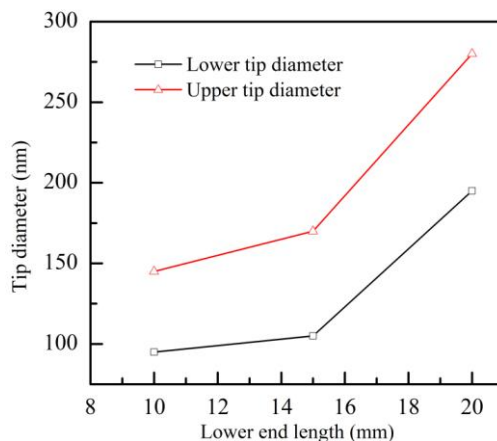


**Figure 12.** Influence of lower-end length on prepared upper and lower nano-electrodes.

### 3.5. Application of nano tips in electromechanical machining

The experimental results indicated that the blunting of the upper tip increased with the cut-off time following breakage of the tungsten rod. With the developed control program, the residual current could be cut off in 5 ms. It is concluded that smaller values of the parameters are preferred for the fabrication of twin nano-electrodes with smaller sizes. As shown in figure 13, twin nano-electrodes with an upper tip of 110 nm in diameter and a lower tip of 80 nm in diameter were fabricated with an applied voltage of 3 V, an electrolyte concentration of 1.5 mol/L, and a lower-end length of 10 mm.

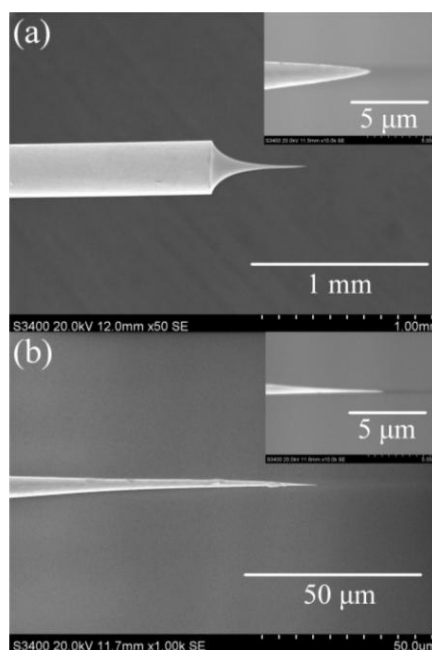


**Figure 13.** Twin nano-electrodes fabricated using the optimum parameters, with an (a) upper tip of 110 nm diameter and (b) a lower tip of 80 nm diameter.

The processed upper and lower nano-electrodes have been applied as tool electrodes in electrochemical micro drilling of micro-holes. Figures 14(a) and (b) show the SEM images of the micro-holes drilled in 2  $\mu\text{m}$  thick nickel plate using upper and lower nano-electrodes. A pulse voltage of 4 V, pulse width of 35  $\mu\text{s}$ , pulse duty ratio of 0.1, and  $\text{H}_2\text{SO}_4$  solution of 0.05 mol/L were used for the electrochemical micro-drilling. Micro-holes of 6 and 2  $\mu\text{m}$  diameter were drilled by feeding the tool electrodes towards the workpiece with a distance of 3  $\mu\text{m}$ .

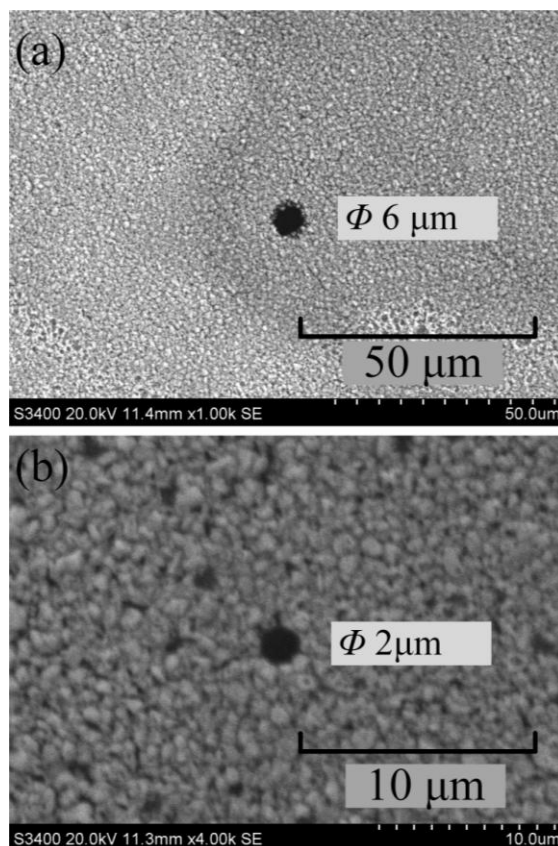


**Figure 14.** Micro-holes of 6 and 3  $\mu\text{m}$  diameter drilled using upper and lower nano-electrodes.

#### 4. CONCLUSIONS

Twin upper and lower nano-electrodes have been fabricated simultaneously using liquid membrane electrochemical etching. After the lower tip drops away, blunting due to residual current increases the diameter of the upper tip, with the blunting being more severe the greater the delay in cutting off the current. The blunting of the upper tip is decreased by the control program developed here, which is able to cut off the residual current in 5 ms. Experimental results show that smaller values of parameters such as applied voltage, electrolyte concentration, and lower-end length are preferred for fabricating twin nano-electrodes with smaller sizes. Appropriate parameters should be selected to avoid low etching efficiency or a boiling effect. Using the developed control method, the

blunting can be decreased with lower voltage and electrolyte concentration. Furthermore, the feasibility of using the fabricated nano-electrodes to drill micro-holes has been shown.

#### ACKNOWLEDGMENTS

This study was supported by the National Natural Science Foundation of China (51375238) and the Jiang Su Natural Science Foundation (BK20131361).

#### References

1. K. P. Rajurkar, M. M. Sundaram and A. P. Malshe, *Procedia CIRP* 6 (2013) 13
2. K. P. Rajurkar, G. Levy, A. Malshe, M. M. Sundaram, J. McGeough, X. Hu, R. Resnick and A. DeSilva, *CIRP Ann. Manuf. Techn.* 55 (2006) 643
3. C. L. Li, D. Y. Fang, X. Li, T. Xue and P. Yao, *Rev. Sci. Instrum.* 83 (2012) 106109
4. E. B. Brousseau, S. S. Dimov and D. T. Pham, *Int. J. Adv. Manuf. Tech.* 47 (2010) 161
5. O. Zinger, P. F. Chauvy and D. Landolt, *J. Electrochem. Soc.* 150 (11) (2003) B495
6. R. Schuster, V. Kirchner, P. Allongue and G. Ertl, *Science* 289 (2000) 98
7. A. L. Trimmer, J. L. Hudson, M. Kock and R. Schuster, *Appl. Phys. Lett.* 82 (2003) 3327
8. M. Kock, V. Kirchner and R. Schuster, *Electrochim. Acta.* 48 (2003) 3213
9. S. H. Ahn, S. H. Ryu, D. K. Choi and C. N. Chu, *Precis. Eng.* 28 (2004) 129
10. B. Ghoshal and B. Bhattacharyya, *J. Mater. Process. Tech.* 222 (2015) 410
11. B. Bhattacharyya, J. Munda and M. Malapati, *Int. J. Mach. Tool. Manu.* 44 (2004) 1577
12. R. Mathew and M. M. Sundaram, *J. Mater. Process. Tech.* 212 (2012) 1567
13. J. P. Ibe, P. P. Bey, S. L. Brandow, R. A. Brizzolara, N. A. Burnham, D. P. Dilella, K. P. Lee, C. R. K. Marrian and R. J. Colton, *J. Vac. Sci. Technol. A* 8 (1990) 3570
14. Y. Khan, H. Al-Falih, Y. Zhang, T. K. Ng and B. S. Ooi, *Rev. Sci. Instrum.* 83 (2012) 063708
15. Y. Ge, W. Zhang, Y. L. Chen, C. Jin and B. F. Ju, *J. Mater. Process. Tech.* 213 (2013) 11
16. A. B. Milhim and R. B. Mrad, *J. Vac. Sci. Technol. B* 32 (2014) 031806
17. H. Chen, W. Xiao, X. Wu and K. Yang, *J. Vac. Sci. Technol. B* 32 (2014) 061801
18. Y. M. Lim and S. H. Kim, *Int. J. Mach. Tool. Manu.* 41 (2001) 2287
19. Y. B. Zeng, X. J. Wu, N. S. Qu and D. Zhu, *Micro and Nanosystems* 5 (2013) 261
20. X. J. Wu, N. S. Qu, Y. B. Zeng and D. Zhu, *Int. J. Adv. Manuf. Tech.* 69 (2013) 723
21. Y. Wang, N. Qu, Y. Zeng, X. Wu and D. Zhu, *Int. J. Precis. Eng. Manu.* 14 (2013) 2179
22. Y. B. Zeng, Y. F. Wang, X. Wu, K. Xu and D. Zhu, *Rev. Sci. Instrum.* 85 (2014) 126105